

Cite this: DOI: 10.1039/xxxxxxxxxx

Inorganic co-crystal formation and thermal disproportionation in a dicyanometallate ‘superperovskite’[†]

Joshua A. Hill,^{a,b} Claire A. Murray,^c Chiu C. Tang,^c Peter M. M. Thygesen,^a Amber L. Thompson^a and Andrew L. Goodwin^{a*}

Received Date
Accepted Date

DOI: 10.1039/xxxxxxxxxx

www.rsc.org/journalname

We report the synthesis, crystal structure, and thermally-driven phase transformation of the dicyanometallate superperovskite co-crystal $[\text{NBu}_4]\text{Mn}[\text{Au}(\text{CN})_2]_3 \cdot [\text{NBu}_4]\text{ClO}_4$. This phase is understandable in terms of the conventional ABX_3 perovskite structure type, but with the NBu_4^+ A-site cation displaced onto the perovskite cage face and 1-dimensional AX' chains included within framework pores opened up by these displacements. On heating to 380 K, the co-crystal disproportionates into its two inorganic components: a bcs-structured ABX_3 phase and $[\text{NBu}_4]\text{ClO}_4$. This system illustrates a new type of structural and phase complexity accessible to dicyanometallate perovskites.

Hybrid perovskites are a populous and important contemporary materials family that couple the functional capabilities of the perovskite structure type with the chemical versatility of hybrid organic/inorganic materials.^{1–5} The incorporation of organic substituents within the ABX_3 perovskite structure tends to increase structural complexity as a result of the increased number of degrees of freedom of molecular vs monoatomic species.^{4,6–11} This additional complexity can have important functional implications. In the now-famous lead halide photovoltaic perovskites, for example, low-energy tumbling of methylammonium cations is thought to assist with exciton stabilisation by preventing recombination.¹² Likewise, molecular orientational order/disorder phase transitions give rise to ferroelectricity and glassy (relaxor-like) dielectric response in various formate perovskites.^{13–16}

The interplay between molecular degrees of freedom and bulk

materials properties is still relatively poorly understood,³ and can be subtle indeed: the emergence of polarisation from coupled quadrupolar orientational order of guanidinium ions and collective Cu^{2+} Jahn-Teller order in $[\text{Gua}][\text{Cu}(\text{HCOO})_3]$ is an obvious example.^{17–19} Consequently, there is a strong need for fundamental studies in the field aimed at understanding exactly what structural and chemical degrees of freedom are accessible to different hybrid perovskites, and how these degrees of freedom might then be exploited in a functional sense.

There are two key reasons why, amongst hybrid perovskites, those based on dicyanometallate $[\text{NC}-(\text{Ag}/\text{Au})-\text{CN}]$ X-site linkers might be expected to exhibit especially unusual and/or complex structural behaviour.²⁰ First, the combination of a metal...metal separation of ~ 1 nm and an atomically-thin anionic linker translates to a particularly large A-site cavity, which can in principle host equally large and structurally complex molecular species. Indeed the aristotypic ABX_3 cell volume of dicyanometallate perovskites is nearly 20 times greater than that of conventional oxide perovskites; hence the moniker ‘superperovskites’.^{20,21} And, second, dicyanometallates are intrinsically ultraflexible solids, capable of extreme mechanical responses to physical and chemical stimuli.^{22–24}

So, as part of a broad investigation into the structural chemistry of dicyanometallate phases,^{20,25} we have taken a particular interest in the phase behaviour of superperovskites. Relatively few are known, and all those that have been identified to date make use of the very large and almost-spherical organic cation PPN^+ on the A-site.^{20,21} Here we describe a new—and, we argue, particularly interesting—superperovskite related instead to $[\text{NBu}_4]\text{Mn}[\text{Au}(\text{CN})_2]_3$. This is an unexpected phase to form because NBu_4^+ usually templates a denser octahedrally-coordinated ABX_3 structure with the bcs topology.^{20,21,26} We will come to show that the perovskite structure type is stabilised in this new system by a most unusual mechanism: namely, the inclusion of an additional inorganic salt as a co-crystal. We used variable-temperature synchrotron X-ray powder diffraction (SXPDP) mea-

^aDepartment of Chemistry, University of Oxford, Inorganic Chemistry Laboratory, South Parks Road, Oxford OX1 3QR, U.K. Tel: +44 (0)1865 272137; E-mail: andrew.goodwin@chem.ox.ac.uk

^bConservation of Wall Painting Department, Courtauld Institute of Art, Somerset House, Strand, London WC2R 0RN, UK

^cDiamond Light Source Ltd., Harwell Science and Innovation Campus, Didcot, Oxfordshire OX11 0DE, UK

[†] Electronic Supplementary Information (ESI) available. See DOI: 10.1039/b000000x/

measurements²⁷ to study the thermal stability of this $ABX_3 \cdot AX'$ phase, and so establish the coupling of compositional and structural degrees of freedom in this unconventional hybrid perovskite.

It was in an attempt to prepare the Mn analogue of bcs-structured $[NBu_4]Ni[Au(CN)_2]_3$ (Ref. 21) that we combined concentrated ethanolic solutions of $[NBu_4]Au(CN)_2 \cdot \frac{1}{2}H_2O$ and $Mn(ClO_4)_2 \cdot xH_2O$. Depending on the rate of mixing, we obtained either single-crystal or polycrystalline samples of the same compound $[NBu_4]Mn[Au(CN)_2]_3 \cdot [NBu_4]ClO_4$ (**1**); this composition was verified by elemental analysis (see SI), and we will come to show it to be supported also by crystal structure determination.

The single-crystal diffraction pattern of **1** was complicated by a large pseudocubic unit cell, on the one hand, and the presence of temperature-dependent structured diffuse scattering, on the other hand [Fig. 1(a)]. Nevertheless, tetragonal crystal symmetry was evident directly from inspection of the raw diffraction data (e.g. different diffuse scattering conditions for $(h0l)/(0kl)$ vs $(hk0)$ planes), and we were able to obtain a good structure solution in the tetragonal space group $P4/ncc$ with refinement statis-

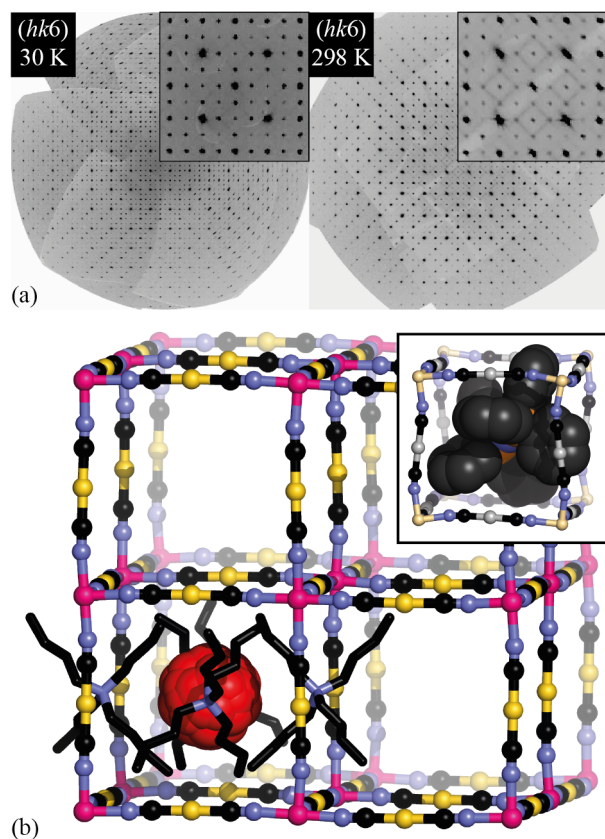


Fig. 1 (a) Representative sections of the single-crystal X-ray diffraction pattern of **1** at 30 K (left) and 298 K (right), demonstrating the evolution of temperature-dependent structured diffuse scattering. The form of this scattering was consistent amongst different crystals. (b) Representation of the crystallographic unit cell of **1**, with extra-framework ions shown for only one superperovskite subcell. The tetragonal axis is vertical. Mn atoms in pink, Au in gold, C in blue, and N in black; H atoms omitted. NBu_4^+ cations are shown in stick representation, and the ClO_4^- anion is disordered over multiple orientations. The inset shows for comparison a representation of the superperovskite subcell of the related system $[PPN]Cd[Ag(CN)_2]_3$.²⁰

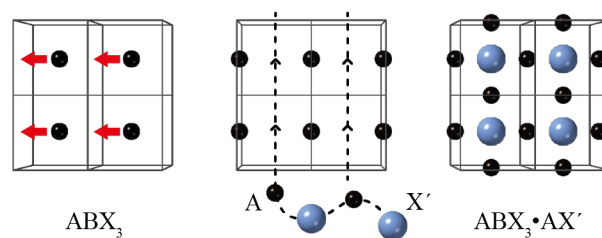


Fig. 2 Schematic illustration of the relationship between ABX_3 and $ABX_3 \cdot AX'$ structure types. The anionic BX_3 framework is shown in stick representation.

tics ($R = 12.6\%$) that are acceptable for a compositionally complex crystal with correlated disorder. The unit cell dimensions of this structure corresponded to a $2 \times 2 \times 2$ supercell of the superperovskite aristotype (i.e. $a, c \simeq 21 \text{ \AA}$).

In our structural model, the anionic $\{Mn[Au(CN)_2]_3\}^-$ framework was crystallographically well-behaved and showed very little sign of complexity [Fig. 1(b)]. By contrast, the remaining electron density was significantly more challenging to interpret as it was distributed over both the conventional perovskite A-site (12-coordinate) and also two-thirds of the 4-coordinate windows of the superperovskite cage. The electron density at this 4-coordinate site was consistent with NBu_4^+ cations; the individual carbon atoms of the pendant alkyl chains were distinguishable in the Fourier maps. The remaining electron density centred at the A-site amounted to $47 e^-$ per site, which is very close to the value anticipated for a single ClO_4^- ion ($50 e^-$). Including a ClO_4^- ion at this site—albeit distributed over a number of symmetry-related orientations (see SI)—gave a structural model with chemical formula $[NBu_4]Mn[Au(CN)_2]_3 \cdot [NBu_4]ClO_4$, which is chemically sensible, charge balanced, and consistent with elemental analysis. In other words, **1** is an inorganic co-crystal of the type $ABX_3 \cdot AX'$.

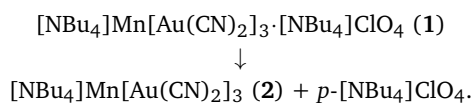
As such, the crystal structure we determined for **1** is closely related to—but meaningfully different from—the conventional perovskite structure type. We understand the relationship in the following way [Fig. 2]. Starting from the hypothetical superperovskite parent $[NBu_4]Mn[Au(CN)_2]_3$, we note that the NBu_4^+ cation is too small for the 12-coordinate site; the analysis of Ref. 28 would suggest a tolerance factor of ~ 0.85 (cf. 0.98 for $[PPN]Mn[Au(CN)_2]_3$; Ref. 20), and hybrid perovskites with NBu_4^+ on the A-site usually require smaller linkers, such as the dicyanamide ion.⁷ Consequently the (relatively) smaller cation is displaced by a half a unit-cell sideways to occupy instead the 4-coordinate windows of the superperovskite cage. This leaves a very open structure that can now accommodate chains of $[NBu_4]ClO_4$, such that these additional NBu_4^+ cations also occupy 4-coordinate sites, and the ClO_4^- ions sit on the 12-coordinate site. The mismatch in local symmetry for the ClO_4^- ions results in substantial orientational disorder; correlations within this disordered state are likely responsible for the observed diffuse scattering.^{29–31}

The crystal structure of the inclusion component $[NBu_4]ClO_4$ does not appear to have been reported previously, but that of the closely related system $[NEt_4]ClO_4$ is known:³² it is rocksalt-

type, and has a $\text{ClO}_4^- \dots (\text{NEt}_4^+) \dots \text{ClO}_4^-$ separation of about 10.7 Å. Importantly, this distance closely matches the characteristic superperovskite cage length ($\sim a/2$), which would explain why $[\text{NBu}_4]\text{ClO}_4$ can be included in **1** in a commensurate manner, in contrast to the incommensurate mechanisms reported for other dicyanometallates.³³ We note that $[\text{NEt}_4]\text{ClO}_4$ also shows extensive room-temperature orientational disorder of both molecular cation and anion, which is consistent with what we observe for **1**. In the case of $[\text{NEt}_4]\text{ClO}_4$, this multi-site disorder appears to preempt the transition to a plastic phase known to occur on heating to 378 K.³⁴

Given the anomalous thermomechanical properties of many other dicyanometallates,^{22,23} we were interested to understand how the structure of **1** evolved with temperature. We used variable-temperature SXPD measurements to probe its structural behaviour over the range 140–480 K; the samples we studied were ground single crystals. For data collected between 140 and 380 K, we were able to fit the diffraction pattern entirely in terms of the $P4/ncc$ model described above [Fig. 3(a)]. The system showed moderate isotropic positive thermal expansion within this regime (see SI for further discussion).

On heating above 380 K, an irreversible phase transition took place that was complete by 410 K [Fig. 3(b)]; thermogravimetric analysis showed no mass loss associated with the transition. The vast majority of the diffraction pattern within this transformed regime could be accounted for by a phase with the **bcs**-type structure of $[\text{NBu}_4]\text{Ni}[\text{Au}(\text{CN})_2]_3$ [Fig. 3(c)];²¹ the obvious candidate for this dominant phase is $[\text{NBu}_4]\text{Mn}[\text{Au}(\text{CN})_2]_3$ (**2**). The component of the diffraction pattern left unaccounted for by this **bcs**-type phase was of much reduced intensity and hence was unlikely to include any Au. This component gave a simple diffraction pattern that was dominated by a low-angle peak corresponding to a d -spacing of ~ 10.5 Å; this pattern could not be indexed in terms of the structures of either **1** or **2**. Instead, samples recovered to room temperature show that this peak had split and matched well the low-angle diffraction features of $[\text{NBu}_4]\text{ClO}_4$ [Fig. 3(c)]. Consequently we tentatively assigned this minority phase within the transformed regime to a plastic form of $[\text{NBu}_4]\text{ClO}_4$, possibly in the CsCl structure. As such, the phase transformation process that occurred at ~ 400 K corresponds to the co-crystal disproportionation³⁵ reaction



We suggest that the driving force for this reaction is the additional entropy gain associated with formation of a plastic phase (p -) of $[\text{NBu}_4]\text{ClO}_4$. The orientational degrees of freedom of both NBu_4^+ and ClO_4^- ions are constrained by the ABX_3 lattice of the crystal structure of **1**, and hence co-crystal disproportionation is required in order to allow molecular tumbling. The superperovskite host left behind is presumably unstable with respect to the **bcs**-structured phase **2** as a result of the smaller effective radius of the NBu_4^+ cation (e.g. vs PPN^+). The fact that this transformation is necessarily reconstructive leaves open the possibility of using kinetic trapping to quench the unstable perovskite-structured

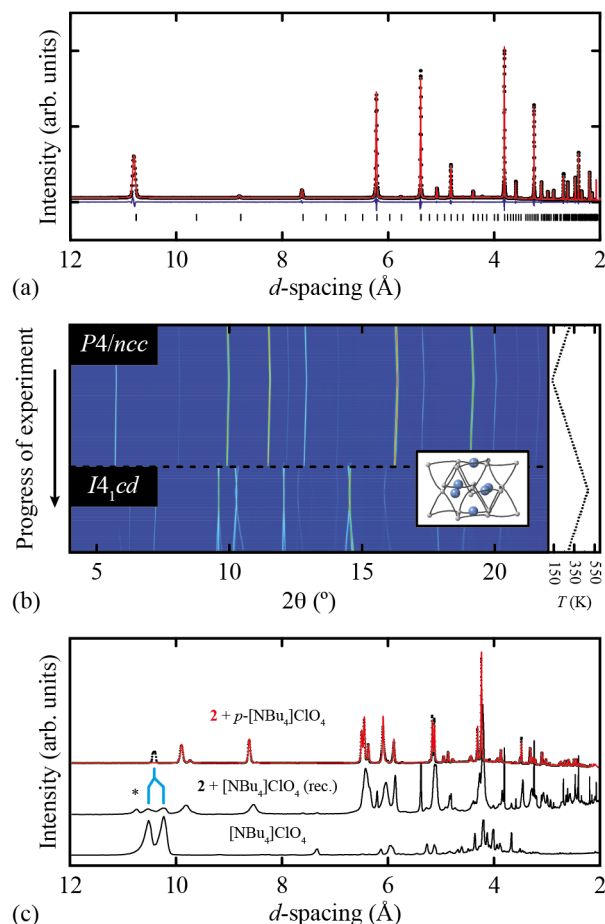


Fig. 3 (a) Ambient-temperature SXPD pattern of **1** (black markers), Pawley fit (red line) and difference (blue line); tick marks indicate calculated reflection positions. (b) Heat-map representation of variable-temperature SXPD patterns during successive cooling–heating–cooling experiments ($\lambda = 1.078265(10)$ Å). Temperature profile is shown to the right, and a schematic representation of the ABX_3 structure of **2** is shown in the inset. (c) High-temperature SXPD pattern (black markers) and corresponding Pawley fit (red line) based on the **bcs** structure of **2** (top). Note the dominant unfitted peak at 10.5 Å. In samples recovered to room temperature (middle) this peak splits, consistent with the ambient-temperature diffraction pattern of $[\text{NBu}_4]\text{ClO}_4$ (bottom). The spurious additional peak marked by an asterisk arises from a very small fraction of unreacted **1** preserved during the recovery experiment.

$[\text{NBu}_4]\text{Mn}[\text{Au}(\text{CN})_2]_3$ intermediate to ambient conditions. Such an approach may be more straightforward if it is possible to use a divalent transition-metal with nonzero crystal field stabilisation energy as the B-site cation. We flag this as a potential avenue for future research.

So what we find in the case of our title compound **1** is that inorganic co-crystal formation acts as a mechanism for stabilising the perovskite structure type. In this sense there is an unexpected parallel to the chemistry of clathrates³⁶ and ion-templated zeolites;^{37,38} it is only when $[\text{NBu}_4]\text{ClO}_4$ is present within the framework structure of $[\text{NBu}_4]\text{Mn}[\text{Au}(\text{CN})_2]_3$ that it assumes a structure related to perovskite. The existence of co-crystalline $\text{ABX}_3 \cdot \text{AX}'$ derivatives now establishes a new type of compositional degree of freedom relevant to this particular branch of hybrid perovskites. Are perchlorate salts the only ones capable of sta-

bilising such phases? If not, how does compositional variation affect phase formation, phase stability, and the kinetics of disproportionation? Moreover, we anticipate that the thermal disproportionation process itself may provide a number of useful and interesting avenues for further research. Specifically, we note that compound **2** is polar (space group $I4_1cd$),²¹ and the ambient phases of most amine perchlorates are ferroelectrics.^{39,40} Consequently the formation of a eutectic during disproportionation of **1** (or its analogues) may provide a novel entry point to controlling functional microstructure in molecular ferroelectrics.

Acknowledgements

The authors gratefully acknowledge funding from the E.R.C. (Grant 279705) and the E.P.S.R.C and useful discussions with M. J. Cliffe, R. I. Cooper, and A. Simonov. This work made use of the I11 and I19 beamlines at the Diamond synchrotron, U.K (experiments EE11544 and MT9981, respectively).

Conflict of interest

There are no conflicts to declare.

References

- 1 D. B. Mitzi, *J. Chem. Soc., Dalton Trans.*, 2001, 1–12.
- 2 A. K. Cheetham and C. N. R. Rao, *Science*, 2007, **318**, 58–59.
- 3 W. Li, Z. Wang, F. Deschler, S. Gao, R. H. Friend and A. K. Cheetham, *Nat. Rev. Mater.*, 2017, **2**, 16099.
- 4 G. Kieslich and A. L. Goodwin, *Mater. Horiz.*, 2017, **4**, 362–366.
- 5 S. Körbel, M. A. Marques and S. Botti, *J. Mater. Chem. A*, 2018, **6**, 6463–6475.
- 6 A. L. Goodwin, *Phys. Rev. B*, 2006, **74**, 134302.
- 7 J. M. Bermúdez-García, M. Sánchez-Andújar, S. Yáñez-Vilar, S. Castro-García, R. Artiaga, J. López-Beceiro, L. Botana, Á. Alegría and M. A. Señaris-Rodríguez, *Inorg. Chem.*, 2015, **54**, 11680–11687.
- 8 S. G. Duyker, J. A. Hill, C. J. Howard and A. L. Goodwin, *J. Am. Chem. Soc.*, 2016, **138**, 11121–11123.
- 9 J. M. Bermúdez-García, M. Sánchez-Andújar, S. Yáñez-Vilar, S. Castro-García, R. Artiaga, J. López-Beceiro, L. Botana, Á. Alegría and M. A. Señaris-Rodríguez, *J. Mater. Chem. C*, 2016, **4**, 4889–4898.
- 10 H. L. B. Boström, J. A. Hill and A. L. Goodwin, *Phys. Chem. Chem. Phys.*, 2016, **18**, 31881–31894.
- 11 L. C. Gómez-Aguirre, B. Pato-Doldán, A. Stroppa, L.-M. Yang, T. Frauenheim, J. Mira, S. Yáñez-Vilar, R. Artiaga, S. Castro-García, M. Sánchez-Andújar and M. A. Señaris-Rodríguez, *Chem. Eur. J.*, 2016, **22**, 7863–7870.
- 12 J. M. Frost and A. Walsh, *Acc. Chem. Res.*, 2016, **49**, 528–535.
- 13 T. Besara, P. Jain, N. S. Dalal, P. L. Kuhns, A. P. Reyes, H. W. Kroto and A. K. Cheetham, *Proc. Natl. Acad. Sci., U.S.A.*, 2011, **108**, 6828–6832.
- 14 N. Abhyankar, J. J. Kweon, M. Orio, S. Bertaina, M. Lee, E. S. Choi, R. Fu and N. S. Dalal, *J. Phys. Chem. C*, 2017, **121**, 6314–6322.
- 15 M. Maczka, N. L. M. Costa, A. Gabor, W. Paraguassu, A. Sieradzki and J. Hanuza, *Phys. Chem. Chem. Phys.*, 2016, **18**, 13993–14000.
- 16 H. L. B. Boström, M. S. Senn and A. L. Goodwin, *Nature Commun.*, 2018, **9**, 2380.
- 17 A. Stroppa, P. Jain, P. Barone, M. Marsman, J. M. Perez-Mato, A. K. Cheetham, H. W. Kroto and S. Picozzi, *Angew. Chem.*, 2011, **50**, 5847–5850.
- 18 A. Stroppa, P. Barone, P. Jain, J. M. Perez-Mato and S. Picozzi, *Adv. Mater.*, 2013, **25**, 2284–2290.
- 19 N. L. Evans, P. M. M. Thygesen, H. L. B. Boström, E. M. Reynolds, I. E. Collings, A. E. Phillips and A. L. Goodwin, *J. Am. Chem. Soc.*, 2016, **138**, 9393–9396.
- 20 J. A. Hill, A. L. Thompson and A. L. Goodwin, *J. Am. Chem. Soc.*, 2016, **138**, 5886–5896.
- 21 J. Lefebvre, D. Chartrand and D. B. Leznoff, *Polyhedron*, 2007, **26**, 2189–2199.
- 22 A. L. Goodwin, M. Calleja, M. J. Conterio, M. T. Dove, J. S. O. Evans, D. A. Keen, L. Peters and M. G. Tucker, *Science*, 2008, **319**, 794–797.
- 23 J. L. Korčok, M. J. Katz and D. B. Leznoff, *J. Am. Chem. Soc.*, 2009, **131**, 4866–4871.
- 24 A. B. Cairns, J. Catafesta, C. Levelut, J. Rouquette, A. van der Lee, L. Peters, A. L. Thompson, V. Dmitriev, J. Haines and A. L. Goodwin, *Nature Mater.*, 2013, **12**, 212–216.
- 25 J. A. Hill, K. E. Christensen and A. L. Goodwin, *Phys. Rev. Lett.*, 2017, **119**, 115501.
- 26 O. D. Friedrichs, M. O’Keeffe and O. M. Yaghi, *Acta Cryst. A*, 2003, **59**, 515–525.
- 27 S. P. Thompson, J. E. Parker, J. Potter, T. P. Hill, A. Birt and T. M. Cobb, *Rev. Sci. Instrum.*, 2009, **80**, 075107.
- 28 G. Kieslich, S. Sun and A. K. Cheetham, *Chem. Sci.*, 2015, **6**, 3430–3433.
- 29 T. R. Welberry and D. J. Goossens, *IUCrJ*, 2014, **1**, 550–562.
- 30 D. A. Keen and A. L. Goodwin, *Nature*, 2015, **521**, 303–309.
- 31 T. R. Welberry and T. Weber, *Cryst. Rev.*, 2016, **22**, 2–78.
- 32 J. Kivikoski, J. A. K. Howard, P. Kelly and D. Parker, *Acta Cryst. C*, 1995, **51**, 535–536.
- 33 A. L. Goodwin, B. J. Kennedy and C. J. Kepert, *J Am Chem Soc*, 2009, **131**, 6334–6335.
- 34 H.-Y. Ye, J.-Z. Ge, Y.-Y. Tang, P.-F. Li, Y. Zhang, Y.-M. You and R.-G. Xiong, *J. Am. Chem. Soc.*, 2016, **138**, 13175–13178.
- 35 G. A. Stephenson, A. Aburub and T. A. Woods, *J. Pharm. Sci.*, 2011, **100**, 1607–1617.
- 36 M. D. Hollingsworth and K. D. M. Harris, in *Comprehensive Supramolecular Chemistry*, ed. D. D. MacNicol, R. Bishop and F. Toda, Pergamon, Oxford, 1996, vol. 6, pp. 177–237.
- 37 E. R. Cooper, C. D. Andrews, P. S. Wheatley, P. B. Webb, P. Wormald and R. E. Morris, *Nature*, 2004, **430**, 1012–1016.
- 38 E. R. Parnham and R. E. Morris, *Chem. Mater.*, 2006, **18**, 4482–4487.
- 39 Q. Pan, Z.-B. Liu, H.-Y. Zhang, W.-Y. Zhang, Y.-Y. Tang, Y.-M. You, P.-F. Fei, W.-Q. Liao, P.-P. Shi, R.-W. Ma, R.-Y. Wei and R.-G. Xiong, *Adv. Mater.*, 2017, **29**, 1700831.
- 40 Y.-Y. Tang, P.-F. Li, W.-Q. Liao, P.-P. Shi, Y.-M. You and R.-G. Xiong, *J. Am. Chem. Soc.*, 2018, **140**, 8051–8059.